Proceedings of the 3rd IFAC Workshop on Automatic Control in Offshore Oil and Gas Production, Esbjerg, Denmark, May 30 - June 1, 2018

Th_B_Regular_Talk.2

Assessment of Flexible Operation in an LNG Plant

Ying Ying Xuan* John Pretlove** Nina Thornhill*

*Department of Chemical Engineering, Centre for Process Engineering, Imperial College London, London, UK
**ABB, Industrial Automation Division, Subsea Technology, Ole Deviks Vei 10, Oslo, Norway

Abstract: Process industries are becoming increasingly reliant on electrical power for reasons of efficiency and sustainability. A large industrial site typically has its own power management system to distribute electricity to the process and to manage electrical contingencies such as partial loss of supply. Recent work has illustrated more flexible alternatives to load shedding whereby an industrial process plant can continue to operate at a lower level making use of available electrical power. This paper presents a way for achieving such flexibility in a Liquefied Natural Gas (LNG) plant. It analyzes the consequences for production of varying the consumed power, and assesses the maximum flexibility within the feasible operating envelope of the process. The study has been conducted by modeling and simulation of an LNG plant using the Linde process with three refrigeration cycles. The results also show the relationships between electrical power consumption and production in terms of production rate and product characteristics. They also show that the vapour-liquid equilibrium plays a crucial role in establishing the operating points and setting the boundaries in which the process has to work. Thus, through the assessment and simulation of an LNG plant, this work demonstrates that flexible operation has benefits over alternatives. It achieves more operating points and therefore adds more flexibility.

Keywords: Flexible Operation, LNG Plant, Energy Distribution, RKS EoS, Vapour-Liquid Equilibrium

1. INTRODUCTION

Large industrial sites typically have their own generation plant, a bi-directional connection to the public electricity supply and an electricity distribution system within the site. Commercial electrical power management systems distribute electricity to the process equipment and manage the export or import of power to or from the public supply. Power management systems also manage the allocation of supply during contingencies, for instance if there is a partial loss of generation or a problem in the public supply. At present, contingency management is done by switching off equipment, known as load shedding. Typically, non-critical equipment is switched off first. However, process equipment may also be shut down to manage the shortage of power. The commercial consequences can be high because a large process can take a long time to restart after a shutdown, which can take two weeks, as in the case of the Angola LNG plant (Vukmanovic and Thomas (2017)) or a month, as in the case of the Gorgon LNG plant (Gloystein and Hogue (2016)).

Recent work (Mohd Noor et al. (2018)) illustrated an alternative to load shedding whereby an industrial process plant can adopt flexible operation, which allows the process to continue operating at a lower level during an electrical contingency making use of any remaining electrical power. For instance, in a compressor station, it might be more desirable if there is a power deficit of 20% to reduce

the power consumption of all compressor motors by 20% than to shut down one in five of them.

The purpose of this paper is to examine how flexible operation could be achieved in a Liquefied Natural Gas (LNG) process following the Linde process as described by Stockmann et al. (2001). Devold et al. (2006) and Lerch (2006) state that LNG plants are heavily electrified and particular, they use electric motors to drive the compressors. Therefore LNG is a good topic of study for this paper. This project aims for obtaining a map of operating points as a function of the available power, so that in case of shortfall of the generated power, the industrial plant can move to its new process set points without putting the process at risk.

The reason for studying LNG is that such sites may be located in remote areas where the public power supply is limited, and therefore they have their own industrial power generation plant (Van der Wal et al. (2005)). Loss of generation in the power plant, or a failure in the public supply such that the site must export its power, could be reasons to operate the LNG plant flexibly so that it makes use of the available power but without shutting down (Heiersted et al. (2001)). A good application of this practice can be allocated for the Floating Liquefying Natural Gas (LFNG) plants, in where the liquefaction is carried out offshore. These installations have the advantages of being flexible in terms of obtaining the gas, removing the need for laying pipelines to the shore, as

mentioned by Won et al. (2014). Nevertheless, they are located offshore, and consequently they need to have their own power generation in the floating plant, like the E-houses structures from ABB (ABB (2018)). Thus, the process solely relies on the power supplied by these E-houses, and therefore, it is crucial that the management of this power is as safe as possible. Its reliability then can be improved by implementing flexibility in the LNG process.

The next section gives a brief review of related literature, and then Section 3 presents the methods used to conduct the study and relevant equations which describe the LNG plant. Section 4 highlights the results, by quantifying the relationships between electrical power consumption and production in terms of product characteristics. It also places constraints by establishing the feasible window of flexible operation of the LNG process. There is a brief discussion which highlights assumptions and addresses questions such as model validation, and the paper then ends with conclusions.

2. BACKGROUND

Power management operations comprise a series of techniques that improve the reliability of the power grid and help save money to industries. As mentioned by Chmielewski (2014) and Harjunkoski et al. (2014), these techniques are useful for implementing the SmartGrid concept in the power grid, so industries also help to maintain stability in the power grid. Harjunkoski et al. (2012) and Mitra et al. (2012) give examples of how power management techniques can be used for reducing the overall consumption of a plant considering the volatility of electricity prices. The mentioned papers, however, are more concerned about the economic optimization of production taking into account the electricity prices rather than the consequences in the process due to a possible change in the available power.

In terms of Industrial Power Management (IPM), the current operation decides and shuts down some equipment, as seen in systems such as the Process Power Management developed by ABB (ABB (2016), Van der Wal et al. (2005)), or the Industrial Load Management System by Honeywell (Honeywell (2015)). In some cases, this equipment shut down might lead to a process stop, so this issue needs to be solved. Some examples for the application of IPM can be seen in the text by Todd et al. (2009), in which load shedding is applied to an aluminum smelter plant for assessing its capability for restoring frequency. That work is experimental rather than analytical, so the process is not modeled, and therefore, it is not possible to obtain a relationship between the available power and the products coming out of the process. Fabozzi et al. (2013) have studied the flexibility of different industrial plants, such as an LNG plant, or a cement plant; but the studies were not quantitative. Thus, the present work analyzes the process plants more in detail and aims for improving the drawback of a possible process stop by adding flexibility to the process.

The Linde LNG process has three refrigeration cycles and the process stream corresponding to the LNG. They exchange heat in three heat exchangers as seen in figure 2 (Stockmann et al. (2001)). A model of an LNG pro-cess comprises mass and energy balances, energy transfer equations, and equations of state. Wang (2013) and Vatani et al. (2014) have analyzed the Linde LNG process for modeling it, so they could calculate the total consumption of the plant. While Wang (2013) did it only for the Linde model, Vatani et al. (2014) modeled five different LNG processes, so they could be compared in terms of electrical consumption. Vatani et al. (2014) highlighted the need for VLE calculations in the refrigeration cycle. The work presented in this paper also formulates a model using VLE calculations, nevertheless, unlike the two mentioned works, it quantifies the impact of varying the electrical consumption, and includes calculations for real mixtures in order to get accurate quantification of said variation on the process.

3. MODELING THE LIQUEFIED NATURAL GAS PROCESS

3.1 Methodology

Figure 1 shows the components of the model. Given the available power, the aim is to determine the operating point of the process, together with the flowrate and composition of the LNG product. The power to the process is delivered by electric motors which drive the refrigeration compressors, which alter the internal energy of the fluids in the refrigeration cycles, and thereby change the pressures and temperature in the LNG process. The motor is assumed to be of high efficiency and to convert almost all the electrical power. Compressors are modeled by using a compressor map considering flowrate, pressure, motor speed and isentropic efficiency; while the process model includes heat and mass balances, heat transfer, and thermodynamic properties of the fluids. There are some assumptions in the model and they, as well as their likely impact on the process, are discussed in section 4.1.
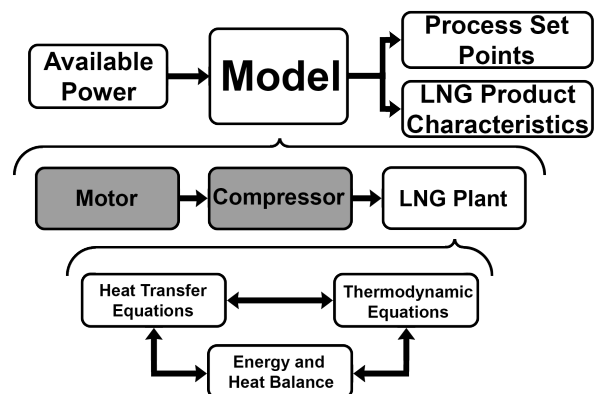
Fig. 1. The model is designed in such a way that it can tell the user to establish a series of set points according to the available power in the plant.

3.2 The LNG Process

The chosen model is an LNG plant using the Linde process as seen in figure 2 (Stockmann et al. (2001)). In this process, the natural gas enters at 30 bars and it undergoes three cooling stages. The refrigerant is compressed and then cooled down to a room temperature, to finally undergo a Joule-Thomson effect for cooling down the natural gas.
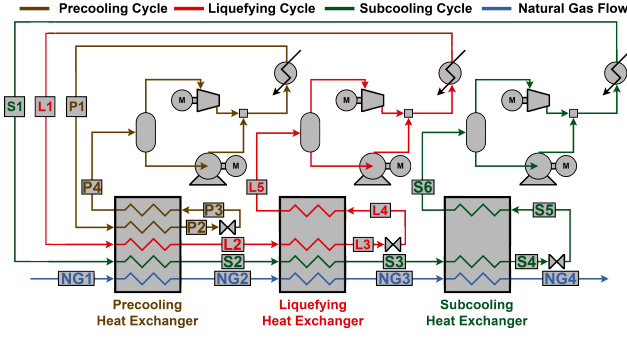
Fig. 2. Liquefied Natural Gas process using the Linde process

The three stages in the process are:

(1) Precooling Cycle: Represented in the diagram with the brown streams, it is responsible to prepare the natural gas for the liquefaction by lowering its temperature to around $-35°C$. This cycle also cools down the remaining refrigerants.

(2) Liquefying Cycle: Represented in the diagram with the red streams, this cycle will lower the natural gas temperature to around $-100°C$. At the end of this stage, the natural gas should be completely liquid. This cycle also cools down the subcooling cycle.

(3) Subcooling Cycle: Represented in the diagram with the green streams, this cycle decreases the natural gas temperature to around $-160°C$.

Ultimately, all the heat absorbed by the refrigerants is released into the sea water.

The following subsection includes the mathematical modeling of the process, including the thermodynamic equations using the Redlich-Kwong Soave (RKS) equations of state, and the heat and mass balances. Most of the following equations are taken from Poling (2007) and Nieto et al. (2013), in which the thermodynamic equations are present. Even so, some equations have to be derived by using thermodynamic properties. The variables and parameters in the equations are defined in the glossary in Appendix A.

3.3 Compressor Power

$$W = H_{out} - H_{in} \qquad (1)$$

This equation shows the consumption of the compressor as the difference of enthalpies between the outlet and the inlet, and it will be used for calculating the necessary power for the plant to operate.

3.4 Thermodynamic Model: RKS Equations

$$P = \frac{RT}{V_m - b} - \frac{a\alpha}{V_m(V_m - b)}$$

$$a = 0.427\frac{(RT_c)^2}{P_c} \qquad b = 0.0866\frac{RT_c}{P_c}$$

$$s = (0.48508 + 1.552\omega - 0.15613\omega^2) \qquad (2)$$

$$\alpha = \left(1 + s\left(1 - \sqrt{\frac{T}{T_c}}\right)\right)^2$$

For a mixture:

$$a\alpha = \sum_{i=1}^{C}\sum_{j=1}^{C} x_i x_j a\alpha_{ij} \qquad b = \sum_{i=1}^{C} b_i x_i \qquad (3)$$

$$a\alpha_{ij} = (1 - k_{ij})\sqrt{a_i a_j \alpha_i \alpha_j}$$

Enthalpies:

$$H = H^{ideal} + H^{Dep}$$

$$H^{ideal} = \sum_i y_i \int_{T_0}^{T} C_{p_i} dT \qquad (4)$$

$$H^{Dep} = (PV_m - RT) - \frac{a\alpha - T\frac{\partial a\alpha}{\partial T}}{b} ln\left(\frac{V_m + b}{V_m}\right)$$

3.5 Thermodynamic Model: Vapour-Liquid Equilibrium

Vapour Liquid distribution ratio

$$K_i = \frac{y_i}{x_i} = \frac{\gamma_i \phi_i^{sat} P_i^{sat} exp\left[\frac{V_m(P - P_i^{sat})}{RT}\right]}{\hat{\phi}_i P} \qquad (5)$$

Rachford-Rice algorithm (only when $T > T_{Bubble}$ and $T < T_{Dew}$:

$$\sum_i \frac{z_i(K_i - 1)}{1 + \psi(K_i - 1)} = 0 \qquad (6)$$

Mass and Energy Balances

$$F_{Prec} = \frac{F_{Liq}(h_{L_2} - h_{L_1}) + F_{Sub}(h_{S_2} - h_{S_1})}{h_{P_1} - h_{P_4}} +$$

$$+ \frac{(H_{NG_2} - H_{NG_1})}{h_{P_1} - h_{P_4}}$$

$$F_{Liq} = \frac{F_{Sub}(h_{S_3} - h_{S_2}) + (H_{NG_3} - H_{NG_2})}{h_{L_2} - h_{L_5}} \qquad (7)$$

$$F_{Sub} = \frac{(H_{NG_4} - H_{NG_3})}{h_{S_3} - h_{S_6}}$$

3.6 Process Analysis

During the analysis, the temperatures at the inlets and outlets of the heat exchangers, and the pressures after the valves are fixed, obtaining then two degrees of freedom, which are used for establishing the available power in the process, and the product characteristics. The equations above are useful for obtaining a series of combinations of set points for the pressure and flowrates given by the compressors as a function of the available power. In addition, there are some constraints that have to be met.

For instance, the compressors have to be modeled not only for determining the surge and choke zone, but also for setting a minimum pressure, which is due to the stream phase when it goes into its respective heat exchanger. If the pressure is significantly below its saturation point, all the latent heat that makes the Joule-Thomson effect possible will not appear, and the stream is going to release heat rather than absorb it. These minimum pressures depend on the composition and the temperatures of the cycle, and they can be seen in figure 3. Every cycle's operating point, when entering its respective heat exchanger, has to be above its respective curve, otherwise, it will release heat instead of absorbing it.
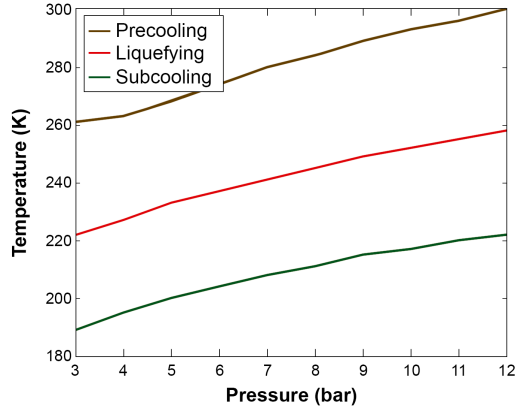
Fig. 3. Minimum pressure of each cycle. The y-axis represents the minimum temperature of the cycle when it enters its respective heat exchanger, and the x-axis represents the minimum pressure provided by the compressor.

4. RESULTS

Figure 1 showed that the process variables are calculated according to the value of the available power. There is not a one-to-one correspondence, meaning that a single work value can give several sets of process variable values, but a single set of process variable values can only give one work value. Due to this inverse one-to-one correspondence, first, the total work is calculated for different process variable values, and then, all the results are mapped, so all series of set points can be found according a single work value.

4.1 Simulations

The model has made the following assumptions:

- All the temperatures are fixed throughout the variable changes, so in the heat exchangers, the streams always absorb or release the necessary amount of energy to reach the desired temperature
- The pressure at the exit of the valve remains constant
- There is no drop pressure due to the piping system
- The valves are isenthalpic, and the rotary machinery is isentropic
- The pressure given by the compressor and the pump in the same cycle is always equal

Due to the first and second assumptions, the phase of the refrigerants at the exit of their respective heat exchangers (P_4, L_5 and S_6 according to figure 2) will be constant, which, during the analysis of this paper, is vapour phase. Thus, the pump is not used in this analysis; however, the code has been tested using it, and it can play a major role for achieving flexible operation in the LNG plant.

4.2 Effects of the Pressure

The text below discusses the impact of the refrigerant cycle pressures on the refrigerant flowrates, highlighting the repercussion of the vapour-liquid equilibrium on them. Due to limited space, this paper shows the results only for the precooling cycle. Analysis of the remaining cycles gives similar results. Figure 4 shows the energy balance in the first heat exchanger, illustrating the state of streams P_1,
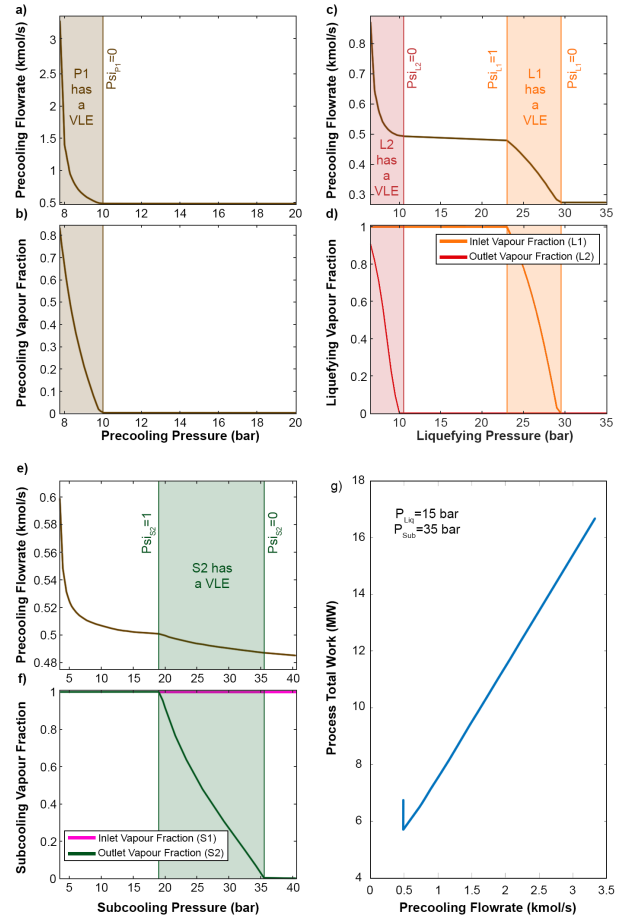
Fig. 4. Influence of the pressure in the precooling cycle flowrate. **a)**, **c)**, and **e)** indicate the flowrate when, respectively, the precooling, the liquefying, and the subcooling pressures vary. **b)**, **d)**, and **f)** show the phases of P_1, L_1 and S_1 (Inlet), and L_2 and S_2 (Outlet) as a function of the pressure.

L_1 and S_1 (Inlet), and L_2 and S_2 (Outlet), following the nomenclature in figure 2. Figures 4.a), c), and e) show how the precooling flowrate is affected by the pressure of each cycle, whereas 4.b), d), and f) indicate the influence of the pressure in the phase of the streams. There is also a strong relationship between the stream phases and the precooling flowrate. To exemplify this, and taking for example figures 4.a), it can be observed that there is a steep variation of the flowrate between 7 and 10 bars, and after that, the flowrate does not notably vary. The reason for this is on figure 4.b), which shows that, between those pressures, P_1 presents a vapour-liquid equilibrium, and it is condensing as the pressure rises, which means that its enthalpy is decreasing as the pressure increases. As mentioned in section 4.1, the refrigerant stream going out of the first heat exchanger has always the same temperature and pressure, consequently, its enthalpy will remain constant. Thus, the enthalpy difference between P_1 and P_4 increases as the pressure rises (both enthalpies are negative). This leads to Eqn.7, which showed that, as the enthalpy difference increases, the flowrate decreases.

When the flowrate stabilizes after reaching a one-phase state, if the pressure increases, the flowrate variation is almost imperceptible, but the rotary machinery needs

more power for reaching that higher pressure, leading to a growing process work. Therefore, the interesting working points are some bars below the transition between having a vapour-liquid equilibrium and having a pure liquid, since, at those areas, the flowrate is arriving to its minimum, and the pressure is not unnecessarily increased.

The final figure, 4.g) shows the total work of the process fixing the liquefying and the subcooling pressures. The horizontal axis represents the flowrate in the precooling cycle, which depends on the pressure in this cycle, and therefore, this graph ultimately shows the total work of the process when the precooling pressure is varied.

4.3 Effects of the Product Characteristics

This section shows how the composition, the temperature and the production rate of the product are affected by the available power. The simulations vary the production rate and the content of methane in the LNG for different LNG temperatures. The temperature at the exit of the process has to be below its saturation point, which is represented with a red line in both figure 5 and 6. Figure 5 shows the influence of the LNG production rate. Since the pressure and composition are the same during the simulation, the saturation point does not vary.

It can be seen that the available power and the production rate have a linear relationship. That is because the enthalpy is an extensive variable, so the rise of heat to be removed due to an increasing production rate, can be solved by increasing proportionly the refrigerant flowrates, and that would imply a proportional increase of the power consumed by the compressors.

Figure 6 shows the influence of the LNG composition on the available power. The simulations varied the methane content, and then varied the rest of components percentage according to the methane change. In this case, the pressure remains constant, but the composition varies, leading to a change in the saturation points indicated by the red line. It can be observed that the greater the methane content, the lower the power consumption. This can be explained considering the low heat capacity of the methane, comparing it to the rest of components present in the natural gas. Observing the red line, the greater the methane content, the lower the saturation point. That is because methane has also a low saturation point.
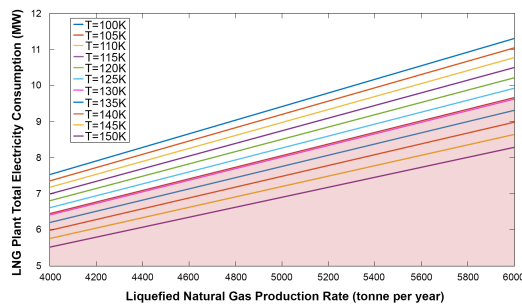
Fig. 5. Influence of the LNG production rate in the available power for different product temperatures. The LNG in this simulation has a 90% mol methane. The operation points have to be above the red zone
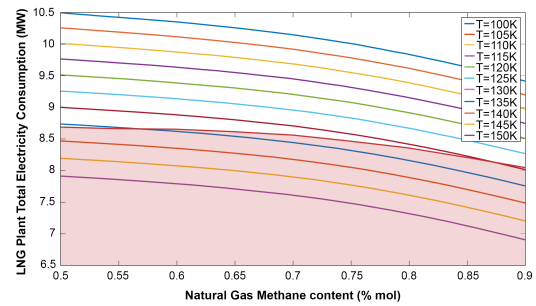
Fig. 6. Influence of the LNG composition in the available power for different product temperatures. The production rate in this simulation is 5000 tonnes per year.

Finally, observing both graphs, it can be seen that the lower the exit temperature, the greater the consumption. It seems to be reasonable, since a lower temperature would imply more heat removal, and therefore, it would also imply either a higher refrigerant flowrate or a higher pressure, which will end up in a higher electricity consumption by the compressors.

5. CONCLUSION

The paper has discussed the advantages of flexible operation for industrial plants with high electricity consumption. The aim of flexible operation is to provide more sophisticated power management, for instance as an alternative to load shedding.

Thus, an assessment of flexible operation in a liquefied natural gas plant has been studied in this article for a production of 5000 tonnes of LNG per year.

All the thermodynamic properties used in this assessment have been modeled for a mixture of real fluids using the Redlich-Kwong Soave equations for a system that is more than susceptible to present vapour-liquid equilibrium. The results show that this equilibrium is a key element for a proper modeling of the LNG process. As can be seen in section 4, during the vapour-liquid equilibrium, a slight change in the pressure supposes a great change in the enthalpy, which in turn will lead to large variations in the flowrate, and thus, in the total power consumption.

Also, the results show that, for a lower consumption in the plant, the pressure has to be maintained some bars below the saturation point. Even so, there is a compromise within that area: if the pressure keeps decreasing, not only the power consumption in the process can drastically rise, but also the process is put at risk. So it is crucial to maintain acceptable levels of pressure, because the process is not rated to operate below the pressures given in figure 3. The results also show that the product characteristics have a great impact on the power consumption.

The overall conclusion is that flexible operation could be implemented in an LNG plant, by varying either the production rate, the refrigerant pressures, the LNG temperature at the exit of the process or the composition of the product. In terms of flexibility, varying the production rate seems to be a more effective approach because it is a more direct operation. However, a proper combination of the four mentioned factors is useful for maintaining the desired level of power consumption within the operating constraints of the process.

ACKNOWLEDGEMENTS

REFERENCES

ABB (2016). ABB Process Power Manager. Ensure a reliable and stable energy supply. [online]. Available at: https://library.e.abb.com/public/5c150d5dd42449d389-5001870f2cfd17/3BNP101100_A_en_ABB_Process_Power_Manager_brochure.pdf. [Accessed 9th March 2018].

ABB (2018). ABB completes the tallest e-houses on a floating LNG facility. [online]. Available at: http://www.abb.com/cawp/seitp202/dc378f554e31766-ec125821c00543369.aspx. [Accessed 9th March 2018].

Chmielewski, D.J. (2014). Smart Grid. The basics - What? Why? Who? How? *AICHE Journal. Chemical Engineering Progress*, August 2014, 28–34.

Devold, H., Nestli, T., and Hurter, J. (2006). All electric LNG plants. Better, safer, more reliable - and profitable. [online]. Available at: https://library.e.abb.com/public/9e770a172afc8d7ec12-5779e004b9974/Paper [Accessed 9th March 2018].

Fabozzi, D., Thornhill, N.F., and Pal, B. (2013). Frequency restoration reserve control scheme with participation of industrial loads. In *2013 IEEE PowerTech Conference, Grenoble*, 1–6.

Gloystein, H. and Hogue, T. (2016). Australia's Gorgon LNG export facility restarting operations. *Reuters*, [online]. Available at: https://de.reuters.com/article/australia-lng-gorgon-chevron/australias-gorgon-lng-export-facility-restarting-operations-chevron-idUKL5N18F204. [Accessed 9th March 2018].

Harjunkoski, I., Bauer, M., and Kymäläinen, T. (2012). Optimal energy management and production scheduling. *Computer Aided Chemical Engineering*, 30, 332–336.

Harjunkoski, I., Scholtz, E., and Feng, X. (2014). Smart Grid. Industry meets the Smart Grid. *Chemical Engineering Progress*, August 2014., 45–50.

Heiersted, R., Jensen, R., Pettersen, R., and Lillesund, S. (2001). Capacity and technology for the Snøhvit LNG plant. In *13 Seoul LNG conference.*

Honeywell (2015). Industrial Load Management System. [online]. Available at: https://www.honeywellprocess.com/library/marketing-/brochures/brochure-on-industrial-load-management-system.pdf. [Accessed 9th March 2018].

Lerch, E. (2006). Full Electrical LNG Plants: Highest Availability and Energy Efficiency through overall System Design. [online]. Available at: http://www.gastechnology.org/Training/Documents/L-NG17-proceedings/Process-3-Edwin_Lerch.pdf. [Accessed 9th March 2018].

Mitra, S., Grossman, I., Pinto, J., and Arora, N. (2012). Optimal production planning under time-sensitive electricity prices for continuous power-intensive processes. *Computers & Chemical Engineering*, 38, 171–184.

Mohd Noor, I., Dawidowski, P., Ottewill, J., and Thornhill, N.F. (2018). Using results from electrical power contingency analysis studies to develop strategies for flexible operation in industrial plants. *Submitted to Applied Energy.*

Nieto, R., González, M., López, I., and Rodríguez, J. (2013). *Termodinámica*. E.T.S.I.I., Madrid; Spain, 2nd edition.

Poling, B.E. (2007). *The Properties of Gases and Liquids*. McGraw-Hill, Boston, [Mass.] ; London, 5th international edition.

Stockmann, R., Forg, W., Bolt, M., Steinbauer, M., Pfeiffer, C., Paurola, P., Fredheim, A., and Sorensen, O. (2001). *Method for Liquefying a Stream Rich in Hydrocarbons*. US Patent 6,253,574.

Todd, D., Caufield, M., Helms, B., Starke, M.R., Kirby, B.J., and Kueck, J.D. (2009). *Providing Reliability Services through Demand Response: A Preliminary Evaluation of the Demand Response Capabilities of Alcoa Inc.* Technical report, United States Department of Energy.

Van der Wal, O., Haugen, T., Holsten, P.E., and Lems, F. (2005). Not on my watch. *ABB Review*, 3, 31–35.

Vatani, A., Mehrpooya, M., and Palizdar, A. (2014). Energy and exergy analyses of five conventional liquefied natural gas processes. *International Journal of Energy Research*, 38(14), 1843–1863. ER-13-3488.R3.

Vukmanovic, O. and Thomas, S. (2017). Angola LNG plant resumes production after December shutdown. *Reuters*, [online]. Available at: https://www.reuters.com/article/angola-lng/angola-lng-plant-resumes-production-after-december-shutdown-idUSL5N1EU211. [Accessed 9th March 2018].

Wang, X. (2013). *Advanced Natural Gas Engineering*. Elsevier Science, Burlington.

Won, W., Lee, S.K., Choi, K., and Kwon, Y. (2014). Current trends for the floating liquefied natural gas (FLNG) technologies. *Korean Journal of Chemical Engineering*, 31(5), 732–743.

Appendix A. GLOSSARY

Variable	Meaning
a, b	RKS equation parameter
c_p	Specific heat capacity (Joules/K mol)
h	Specific enthalpy (Joules/mol)
K_i	Vapour Liquid distribution ratio of component i
k_{ij}	Binary parameter between components i and j
P	Pressure (bar)
T	Temperature (K)
V_m	Molar volume (mol/m^3)
x	Liquid composition
y	Vapour composition
z	Overall composition
W	Work (Watt)
α	RKS equation parameter
γ	Activity coefficient
ω	acentric factor
ϕ	Fugacity coefficient
ψ	Vapour fraction